African Journal of Advanced Pure and Applied Sciences (AJAPAS)
Online ISSN: 2957-644X
Volume 5, Issue 2, 2026
Page No: 51-63
Website: *https://aaasjournals.com/index.php/ajapas/index*
ISI 2025: 1.126 **SJIFactor 2024: 6.752** **معامل التأثير العربي: 1.62**

In-Silico Investigation of Selected Phytochemicals as Potential Androgen Receptor Modulators: A Molecular Docking and ADMET Study

Esmaeil Belead Musa [1*], Abdulaziz Sh. Suwaydan [2], Mhmoud Ali Zughdani [3], Aya Khaled Hadia [4], Duaa Mohammed Alyseer [5], Fatimah Alsanousi Bilhajjah [6], Samiran Sadhukhan [7]

[1] Department of Biomedical Sciences, Faculty of pharmacy, Elmergib University, Al-Khoms, Libya

[2,3,4] Department of Pharmacognosy, Faculty of pharmacy, Elmergib University, Al-Khoms, Libya

[5,6] Last year Pharmacy Students, Department of Biomedical Sciences, Faculty of pharmacy, Elmergib University, Al-Khoms, Libya

[7] Department of Pharmaceutical Chemistry, Netaji Subhas Chandra Bose Institute of Pharmacy, Chakdaha, Ndia, West Bengal, India

دراسة حاسوبية (*In Silico*) لمركبات نباتية مختارة كمعدِّلات محتملة لمستقبل الأندروجين: دراسة الإرساء الجزيئي (*Molecular Docking*) وخصائص الامتصاص والتوزيع والأيض والإطراح والسمّية (*ADMET*)

إسماعيل بلعيد موسى [1*]، عبد العزيز شرف الدين سويدان [2]، محمود علي الزغداني [3]، اية خالد هدية [4]، دعاء محمد اليسير [5]، فاطمة السنوسي بلحاجة [6]، ساميران صادوخا [7]

[1] قسم العلوم الطبية الحيوية، كلية الصيدلة، جامعة المرقب، الخمس ، ليبيا

[4،3،2] قسم علم العقاقير، كلية الصيدلة، جامعة المرقب، الخمس، ليبيا

[6،5] طلبة الصيدلة السنة الأخيرة، قسم العلوم الطبية الحيوية، كلية الصيدلة، جامعة المرقب، الخمس، ليبيا

[7] قسم الكيمياء الصيدلانية، معهد نيتاجي سوباز تشاندرا بوز للصيدلة، تشاكداها ناديا، ولاية غرب البنغال، الهند

[*]Corresponding author: ebmusa@elmergib.edu.ly

Received: January 10, 2026	Accepted: April 03, 2026	Published: April 20, 2026

Abstract:
The Androgen Receptor (AR) is a fundamental therapeutic target for hormone-sensitive diseases, including prostate cancer. This study employed a computational workflow to evaluate the binding potential of five selected phytochemicals—Quercetin, Ursolic acid, β-sitosterol, Berberine, and Rutin—against the human AR (PDB ID: 2AMB). Ligand and receptor preparation were performed using Discovery Studio, while text editing and parameter adjustment were facilitated through Notepad++. Molecular docking was conducted using AutoDock Vina, and molecular visualization and interaction analysis were carried out with PyMOL. Docking results demonstrated that Quercetin and Berberine exhibited the most favorable binding energies of −8.8 kcal/mol and −8.7 kcal/mol, respectively, indicating strong binding affinity for the AR pocket. Evaluation of drug-likeness using Lipinski's and Veber's rules revealed that Quercetin and Berberine comply with pharmacokinetic criteria, whereas Ursolic acid, β-sitosterol, and Rutin showed multiple violations. ADMET predictions further identified Quercetin as possessing favorable oral absorption and metabolic profiles. Detailed molecular interaction analysis elucidated the key amino acid residues stabilizing the ligand within the AR binding pocket. These findings support and underscore supporting the identification of Quercetin as the most promising lead compound for AR modulation, providing a computational foundation for subsequent in vitro and in vivo investigations to validate Quercetin as a potential AR modulator.

Keywords: Prostate Cancer, Androgen Receptor (AR), Phytochemical docking, Quercetin, Berberine.

الملخص

يُعدّ مستقبل الأندروجين (AR) هدفًا علاجيًا أساسيًا في الأمراض الحساسة للهرمونات، بما في ذلك سرطان البروستاتا. هدفت هذه الدراسة إلى استخدام نهج حاسوبي متكامل لتقييم قابلية ارتباط خمس مركبات فيتوكيميائية منتقاة - وهي الكويرسيتين، وحمض الأورسوليك، وبيتا-سيتوستيرول، والبربيرين، والروتين - مع مستقبل الأندروجين البشري (PDB ID: 2AMB). تم تحضير المركبات والبروتين باستخدام برنامج Discovery Studio، في حين أُجري تحرير النصوص وضبط المعاملات باستخدام برنامجNotepad++ . كما تم إجراء دراسات الالتحام الجزيئي باستخدام برنامج AutoDock Vina، بينما استُخدم برنامج PyMOL في التصوير الجزيئي وتحليل التفاعلات. أظهرت نتائج الالتحام الجزيئي أن مركبي الكويرسيتين والبربيرين حققا أفضل طاقات ارتباط بلغت −8.8 و−8.7 كيلو كالوري/مول على التوالي، مما يدل على ألفة ارتباط عالية داخل جيب الارتباط لمستقبل الأندروجين. كما بيّن تقييم قابلية الدواء وفقًا لقواعد ليبينسكي وفيبر أن الكويرسيتين والبربيرين يتوافقان مع المعايير الحركية الدوائية، في حين أظهرت المركبات الأخرى - حمض الأورسوليك، وبيتا-سيتوستيرول، والروتين - عدة مخالفات لهذه القواعد. وأظهرت تنبؤات ADMET كذلك أن الكويرسيتين يتمتع بخصائص امتصاص فموي جيدة وملف أيضي ملائم. وقد كشف التحليل التفصيلي للتفاعلات الجزيئية عن الأحماض الأمينية الرئيسية المسؤولة عن تثبيت المركبات داخل جيب الارتباط لمستقبل الأندروجين. وتدعم هذه النتائج بقوة تحديد الكويرسيتين بوصفه المركب الرئيسي الأكثر وعدًا لتنظيم مستقبل الأندروجين، كما توفر أساسًا حاسوبيًا متينًا لإجراء دراسات لاحقة مخبرية (in vitro) وداخل الكائن الحي (in vivo) للتحقق من فعاليته كعُدل محتمل لهذا المستقبل.

الكلمات المفتاحية: سرطان البروستاتا، مستقبل الأندروجين (AR)، الالتحام الجزيئي للمركبات النباتية، الكويرسيتين، البربيرين.

Introduction

Background on The Androgen Receptor (AR)

The Androgen Receptor (AR) [1] functions as a ligand-dependent transcription factor belonging to the nuclear receptor superfamily, activated by androgen hormones (e.g., testosterone, dihydrotestosterone) [2]. It is expressed in various tissues, including the prostate, skeletal muscle, liver, and central nervous system, where it mediates the physiological effects of androgens [3]. Upon activation, the AR regulates gene expression, playing a vital role in the development and maintenance of male secondary sexual characteristics [4]. Dysregulation of the AR signaling pathway is implicated in diseases such as benign prostatic hyperplasia and prostate cancer [5]. Structurally, the AR is encoded by the AR gene located on the X chromosome (Xq11-12) and consists of approximately 919 amino acids [6]. Its modular architecture includes three major domains: the intrinsically disordered N-terminal domain (NTD), the central DNA-binding domain (DBD), and the C-terminal ligand-binding domain (LBD). The NTD harbors the transcriptional activation function-1 (AF-1), which is essential for coactivator recruitment and transcriptional regulation. The DBD contains two zinc finger motifs that facilitate specific binding to androgen response elements (AREs) within the promoter regions of androgen-regulated genes, while the LBD mediates ligand recognition and receptor dimerization through the activation function-2 (AF-2) surface [7]. Upon binding to natural ligands such as testosterone or dihydrotestosterone (DHT), the AR undergoes a series of conformational changes. These include dissociation from cytoplasmic chaperone proteins such as heat shock proteins (HSP70, HSP90), receptor phosphorylation, and subsequent homodimerization. The activated receptor complex then translocates into the nucleus, where it binds to specific DNA sequences known as androgen response elements [8], where it binds ARE sequences and recruits transcriptional coregulators, including coactivators and corepressors. This complex network of protein–protein interactions ultimately modulates the transcription of genes involved in cell proliferation, differentiation, and apoptosis [9]. The AR is tightly regulated through several post-translational modifications, including phosphorylation, acetylation, methylation, and ubiquitination, which modulate its stability, localization, and transcriptional activity [10, 11]. Crosstalk with intracellular signaling cascades, particularly the PI3K/Akt, MAPK, and Wnt/β-catenin pathways, further influences AR function. This cross-regulation enables the receptor to remain active even in low androgen environments—a key mechanism contributing to castration-resistant prostate cancer (CRPC). Furthermore, mutations within the AR gene, amplification of AR expression, and ligand-independent activation by growth factors are known mechanisms underlying therapeutic resistance to antiandrogen therapies, such as bicalutamide and enzalutamide [12-14].

In the context of prostate cancer, aberrant AR signaling promotes tumor cell survival and proliferation. Elevated AR expression has been correlated with higher Gleason scores and more aggressive disease phenotypes. Notably, AR splice variants, such as AR-V7, lack the ligand-binding domain but retain transcriptional activity, allowing cancer cells to bypass androgen deprivation. These variants are considered major contributors to therapy resistance and poor prognosis [15, 16].

Beyond oncology, AR signaling also plays critical roles in metabolic regulation, skeletal muscle hypertrophy, bone density maintenance, and immune modulation. Dysregulation of AR expression has been implicated in disorders such as Kennedy's disease (spinal and bulbar muscular atrophy) and androgen insensitivity syndrome (AIS). The pleiotropic nature of AR function underscores the complexity of targeting this receptor pharmacologically [17-20]. Anti-androgens, which block AR activation, are standard treatments, but resistance often develops. A major challenge in treating prostate cancer is that resistant tumors often exhibit persistent or enhanced AR signaling, though the underlying molecular mechanisms for this remain largely unclear [21, 22]. From a drug discovery perspective, understanding AR structure-function relationships has facilitated rational design of selective AR modulators (SARMs) and has encouraged exploration of natural products with potential antiandrogenic activity. Molecular docking and dynamics studies have revealed that certain phytochemicals—such as flavonoids and alkaloids—can effectively interact with the AR ligand-binding pocket, mimicking or antagonizing endogenous androgens. These findings offer new opportunities for developing safer, naturally derived AR modulators to address the limitations associated with conventional therapies.

Rationale for Phytochemical Screening

Natural products have long been recognized as a rich source of therapeutic agents, with phytochemicals (plant-derived compounds) offering extensive structural diversity, biocompatibility, and multitarget pharmacological potential. Their relatively low toxicity compared to synthetic drugs further enhances their value in drug discovery. In this context, computational approaches, particularly *in silico* screening methods such as molecular docking and ADMET prediction, provide a cost-effective and time-efficient strategy for the early identification of bioactive compounds with favorable pharmacokinetic properties. By enabling the simulation of receptor–ligand interactions alongside the prediction of absorption, distribution, metabolism, excretion, and toxicity profiles, these methodologies significantly improve the efficiency and precision of the drug discovery pipeline. Among the wide range of bioactive phytochemicals, Quercetin, a flavanol widely distributed in fruits, vegetables, and medicinal plants, exhibits potent antioxidant, anti-inflammatory, and anticancer properties [23, 24]. Ursolic acid, a pentacyclic triterpenoid found in apple peels, rosemary, and basil, has attracted interest for its anti-inflammatory, antiproliferative, and hepatoprotective activities [25]. It interacts with multiple signaling pathways, including NF-κB and PI3K/Akt, and exhibits notable affinity toward steroid hormone receptors [26, 27]. β-sitosterol, a plant sterol structurally similar to cholesterol, exhibits anti-inflammatory, immunomodulatory, and anticancer effects [28, 29]. It has been reported to modulate membrane-associated receptor function and inhibit tumor proliferation through induction of apoptosis and regulation of hormonal signaling [29, 30]. Its high binding affinity for hydrophobic protein cavities makes it a frequent hit in docking studies, particularly for steroid-related receptors. Berberine, an isoquinoline alkaloid isolated from *Berberis* species, has long been recognized for its antimicrobial, antidiabetic, and anticancer properties [31-33]. In *in silico* docking studies, Berberine often exhibits strong binding affinities toward enzymes and receptors involved in metabolic and proliferative pathways. Rutin, a glycosylated derivative of Quercetin, demonstrates antioxidant, vasoprotective, and anti-inflammatory effects [34, 35]. Collectively, these structurally diverse and biologically active compounds represent promising candidates for computational investigation as modulators of the Androgen Receptor. Their evaluation through integrated in silico approaches not only facilitates the elucidation of interaction mechanisms at the molecular level but also supports the rational prioritization of lead compounds for subsequent experimental validation, thereby strengthening the link between natural product chemistry and modern drug discovery strategies.

Material and methods

In the present study, we performed computational analyses using well-established and validated software platforms and databases, including PyRx (AutoDock Vina), PyMOL (version 2.5), and Discovery Studio Visualizer, SwissADME, pkCSM, and Pro Tox III, to ensure the methodological reliability and reproducibility of the findings.

1. Receptor and Ligand Preparation

1.1 Receptor Preparation

The three-dimensional (3D) crystal structure of the human Androgen Receptor (AR) (PDB ID: 2AMB) was obtained in PDBx/mmCIF format from the Protein Data Bank (PDB) (https://www.rcsb.org/), a globally recognized database of experimentally determined biomolecular structures, where additional information about the receptor is summarized in Table 1.

Table 1. Selected human receptor proteins with PDB ID, method, and resolution.

Receptor	PDB ID	Organism	Method	Resolution
Androgen Receptor (AR)	2AMB	Homo sapiens	X-ray diffraction	1.75 Å

Prior to docking, the receptor structure was initially examined for missing residues, alternate conformations, and bound water molecules using PyMOL (version 2.5) and Discovery Studio Visualizer. To prepare the receptor for docking, all co-crystallized ligands, ions, and water molecules were removed to eliminate non-essential interactions that might interfere with ligand binding. Subsequently, polar hydrogen atoms were then added to ensure proper representation of hydrogen-bond donors and acceptors, as well as appropriate electrostatic interactions under physiological pH conditions. Gasteiger partial charges were then assigned to all atoms using AutoDock Tools (ADT) to account for electronic distribution across the receptor, a necessary step for accurate molecular docking simulations. To define the docking site, the active site residues were identified from the original ligand-binding cavity in the crystal structure and confirmed by literature references to the androgen receptor's ligand-binding domain, or by using PrankWeb (Figure 1). Using PrankWeb, the active site was further characterized by selecting the pocket with the highest predicted score (48.64) and probability (0.974), which ranked number one among all identified pockets. This binding pocket comprises 19 residues, which, in sequential order, include leucine701 (LEU), leucine704 (LEU), asparagine 705(ASN), leucine707 (LEU), glycine708 (GLY), glutamine 711(GLN), tryptophan 741(TRP), methionine742 (MET), methionine745 (MET), valine 746(VAL), methionine749 (MET), arginine752 (ARG), phenylalanine764 (PHE), methionine 780(MET), methionine 787(MET), leucine873 (LEU), phenylalanine876 (PHE), tryptophan 877(TRP), and leucine880 (LEU), contributing to the structural and functional integrity of the binding site. The geometric center of this pocket is located at coordinates (X = 26.8478, Y = 1.9905, Z = 4.4481), providing a precise reference for subsequent grid box construction and docking studies. This structural model represents the ligand-binding domain of the AR in complex with a co-crystallized ligand and serves as a reliable structural template for subsequent computational docking analyses. A grid box was constructed to encompass this binding pocket with sufficient margin to allow full ligand flexibility and exploration of neighboring sub-pockets. The processed receptor model and its native ligand were subsequently saved in PDBQT format separately, which encodes atom types, coordinates, and charge information compatible with AutoDock or AutoDock Vina docking software.

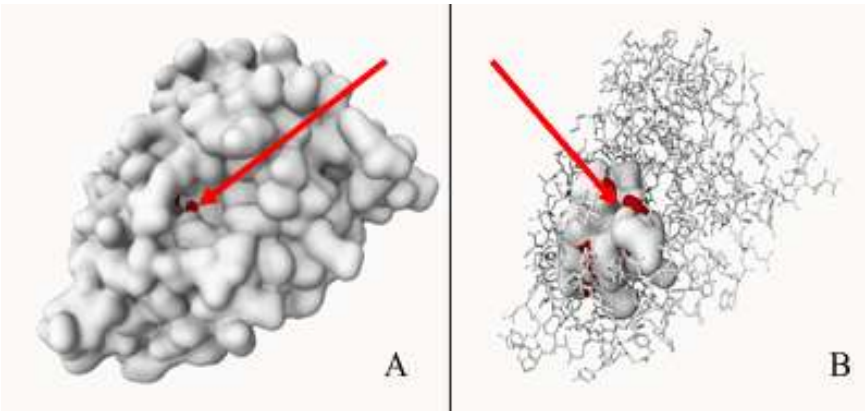

Figure 1: The ligand-binding cavity, highlighted in red, is visualized using (A) a molecular surface model and (B) a ball-and-stick representation.

1.2 Ligand Preparation

The phytochemical ligands selected for this study were retrieved from the PubChem database using their respective Compound Identification Numbers (CIDs) and SMILES structures (https://pubchem.ncbi.nlm.nih.gov/), Table 2. Each compound's 3D structure was downloaded in SDF (Structure Data File) format as well, edited with Notepad^{++}, and subsequently, all ligands were assembled into a single SDF file to facilitate batch processing and simultaneous docking in AutoDock, ensuring consistent preparation across the dataset. Each ligand structure was energy-minimized to optimize bond lengths, angles, and torsions, thereby achieving a stable conformation with the lowest possible potential energy. This step ensures that docking simulations are based on geometrically and energetically realistic molecular structures, converted to PDB format using molecular modeling software, e.g., Open Babel (v3.1.1) for preprocessing. All ligands were then protonated at physiological pH (7.4), and Gasteiger charges were assigned to ensure consistency with receptor electrostatics. Rotatable bonds were automatically detected, allowing torsional flexibility during docking, except for rigid functional groups such as aromatic rings or amide bonds. Each minimized ligand structure was then converted into PDBQT format, which encodes atomic coordinates, torsional degrees of freedom, and partial charges for use in docking algorithm simulations.

Table 2: phytochemicals PubChem CIDs and SMILES

Name	PubChem CID	SMILES
Quercetin	5280343	C1=CC(=C(C=C1C2=C(C(=O)C3=C(C=C(C=C3O2)O)O)O)O)O
Ursolic acid	64945	C[CH]1CC[C]2(CC[C]3(C(=CC[CH]4[C]3(CC[CH]5[C]4(CC[CH](C5(C)C)O)C)C)[CH]2[CH]1C)C)C(=O)O
β-sitosterol	222284	CC[CH](CC[CH](C)[CH]1CC[CH]2[C]1(CC[CH]3[CH]2CC=C4[C]3(CC[CH](C4)O)C)C)C(C)C
Berberine	2353	COC1=C(C2=C[N+]3=C(C=C2C=C1)C4=CC5=C(C=C4CC3)OCO5)OC
Rutin	5280805	C[CH]1[CH]([CH]([CH]([CH]([CH](O1)OC[CH]2[CH]([CH]([CH]([CH](O2)OC3=C(OC4=CC(=CC(=C4C3=O)O)O)C5=CC(=C(C=C5)O)O)O)O)O)O)O)O

1.3 Quality Check and Structure Validation

Visual inspection of both receptor and ligand files was carried out using PyMOL and Discovery Studio Visualizer software to verify structural integrity, proper geometry, charge distribution, and absence of steric clashes or missing atoms. Any discrepancies were corrected before proceeding to the docking phase. The prepared receptor and ligand files were validated by checking for missing atoms, incorrect valencies, or structural inconsistencies before proceeding to the docking phase.

2. Molecular Docking Protocols

2.1. Molecular Docking Software

Molecular docking simulations were performed using AutoDock Vina (version 1.2.0), a robust docking engine that employs a hybrid scoring function combining empirical free-energy and knowledge-based potentials. Docking was performed under default parameters unless otherwise specified.

2.2. Grid Box and Search Space Definition

The grid box was defined in the Pyrex to include the androgen receptor's ligand-binding domain (LBD) pocket, as identified earlier in the 2AMB crystal structure using PrankWeb. with a center at coordinates X = 26.8478, Y = 1.9905, and Z = 4.4481, and dimensions of 25 × 25 × 25 Å, precisely centered on the co-crystallized ligand binding site to ensure full coverage of the active cavity. This configuration enabled flexible ligand exploration and accurate prediction of binding pose. Furthermore, these parameters were optimized to enable efficient and simultaneous molecular docking runs in AutoDock Vina, ensuring smooth achievement and consistent grid alignment across all ligands Table 3.

Table 3: AutoDock Vina grid box parameters for molecular docking.

PDB ID	Vina Search Space					
	Center			Dimensions (Å)		
	X	Y	Z	X	Y	Z
2AMB	26.8478	1.9905	4.4481	25	25	25

2.3 Docking Parameters

Each ligand was docked independently within one file, one after the other, to the prepared androgen receptor model using AutoDock Vina in PyRx. The exhaustiveness parameter, which controls the search depth and determines how thoroughly the conformational space is explored, was set to 32 to ensure thorough conformational sampling and improve docking accuracy. The number of output conformations was set to nine (9) per ligand. Among the generated poses, the one with the lowest predicted binding energy (kcal/mol) was automatically selected by the software as the most favorable binding orientation for subsequent visualization and interaction analysis.

Results and discussion

1. Binding Energy, Affinity, and Docking Analysis

Docking results were ranked based on binding affinity scores (ΔG, kcal/mol) generated by AutoDock Vina. The lowest-energy conformation for each ligand was analyzed for its binding orientation and molecular interactions within the AR receptor's active site Table 4.

Table 4: Binding energies (in kcal/mol) of selected phytochemicals against AR.

PDB ID	Binding energy of ligands (kcal/mol)				
	Quercetin	**Ursolic acid**	**Beta-sitosterol**	**Berberine**	**Rutin**
2AMB	-8.8	+1	-6.1	-8.7	-5.8

2 Output and Visualization

The final binding poses and interaction patterns of Quercetin and Berberine—identified as the ligands exhibiting the lowest binding energies—were subsequently examined and visualized in PyMOL to characterize their interactions with the active-site residues of the androgen receptor (Figure 2). Whereas the remaining phytochemicals (Ursolic acid, β-sitosterol, and Rutin) demonstrated weak or non-ideal binding profiles and displayed unfavorable interactions within the receptor's active site.

3. Molecular Interactions

Two-dimensional (2D) interaction diagrams of Quercetin and Berberine were generated using BIOVIA Discovery Studio Visualizer (Figure 3) to illustrate their specific interactions, presenting the most acceptable binding poses through which these phytochemicals may modulate the androgen receptor (Figure 4. Key non-covalent interactions, including hydrogen bonds, hydrophobic contacts, π–π stacking, and electrostatic interactions, are summarized in Table 5.

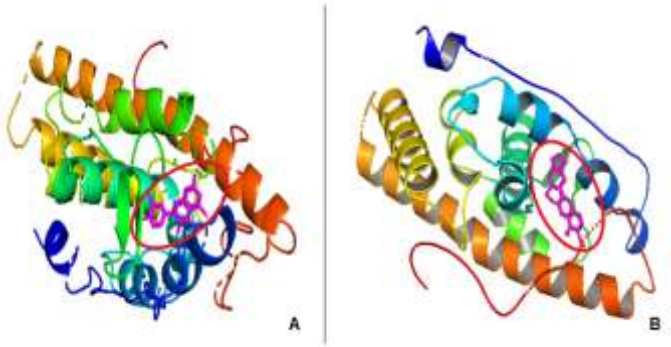

Figure 2: illustrates the positioning of (A) Quercetin and (B) Berberine within the AR binding pocket.

Table 5: presents the hydrogen bonds and additional interactions formed with the amino acid residues within the androgen receptor's binding pocket.

Ligand	Hydrogen bond	Other Interactions
Quercetin	*LEU 704, ASN 705, MET 745*	*LEU 701, LEU 707, GLY 708, VAL 746, ALA 748, MET 749, ARG 752, PHE 764, SER 778, MET 787, LEU 873, PHE 876, THR 877, LEU 880*
Ursolic acid	*LEU 701, ARG 752*	*LEU 704, LEU 707, MET 742, MET 745, MET 749, PHE 764, LEU 873, PHE 876,*
β-sitosterol	//////////////////////	*LEU 701, LEU 704, ASN 705, LEU 707, GLY 708, MET 742, MET 745, MET 749, ARG 752, PHE 764, PHE 770, SER 778, ARG 779, TYR 781, GLN 783, CYS 784, MET 787, LEU 873, PHE 875, THR 877*
Berberine	*ARG 752*	*LEU 701, LEU 704, ASN 705, LEU 707, GLY 708, MET 745, VAL 746, MET 749, PHE 764, MET 787, LEU 873, PHE 876, THR 877, LEU 880*
Rutin	*LEU 701, ASN 705, MET 745, PHE 764, THR 877*	*LEU 704, LEU 707, GLY 708, TRP 741, MET 742, VAL 746, MET 749, ARG 752, ALA 765, CYS 784, MET 787, LEU 873, PHE 876, LEU 880, VAL 889, PHE 891, ILE 899,*

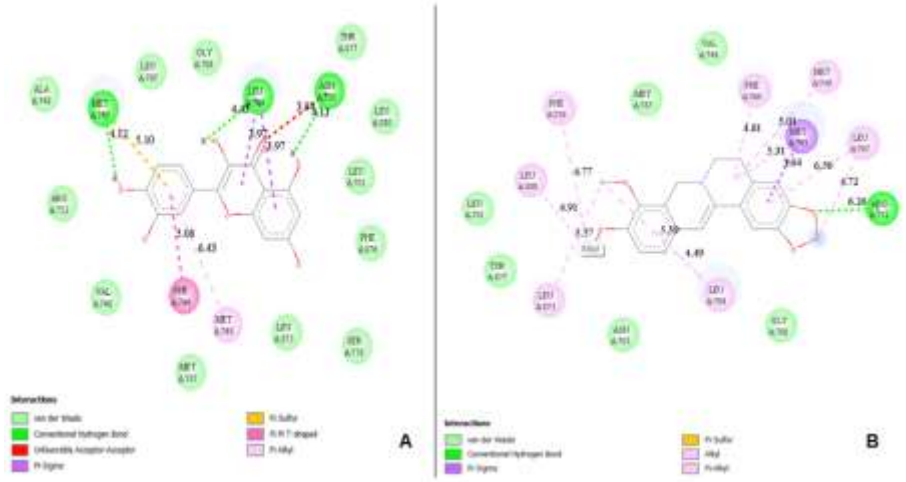

Figure 3: Two-dimensional (2D) interaction of AR binding cavity shown as (A) Quercetin: (B) Berberine.

4. Drug-likeness and Pharmacokinetics (ADME)

The physicochemical properties of each compound—including molecular weight (MW), number of rotational bonds (NRB), hydrogen bond donors (HBD), hydrogen bond acceptors (HBA), lipophilicity (LogP), and topological polar surface area (TPSA)—were calculated using their SMILES through the SwissADME web server (https://www.swissadme.ch/). These parameters were evaluated according to Lipinski's Rule of Five (MW ≤ 500 Da, LogP ≤ 5, HBD ≤ 5, HBA ≤ 10) and Veber's Rule (TPSA ≤ 140 Å², NRB ≤ 10) to predict oral bioavailability and assess drug-likeness. In accordance with Lipinski's guidelines, compounds meeting these criteria were considered drug-like, whereas violations were recorded; molecules exhibiting no more than one violation were classified as potentially drug-like and androgen receptor modulators Table 6.

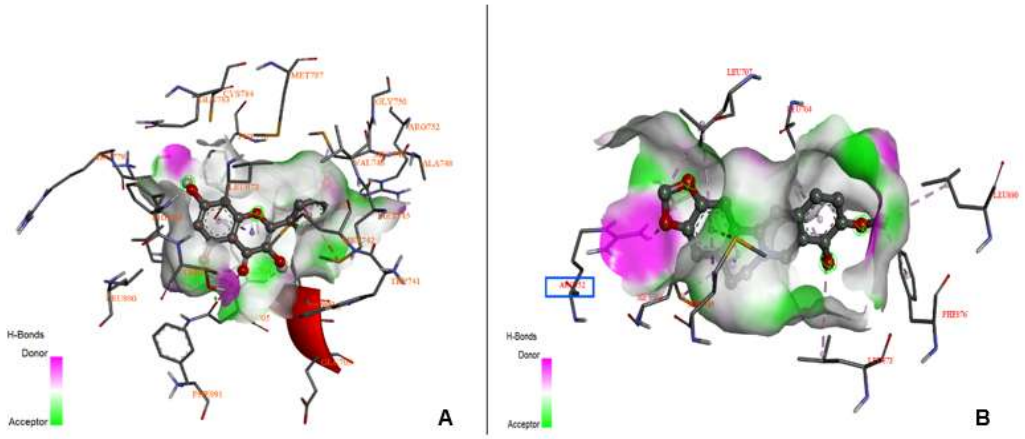

Figure 4: depicts the 3D structures of (A) Quercetin and (B) Berberine positioned within the androgen receptor binding pocket

Table 6: Drug-likeness properties of molecules based on Lipinski's and Veber's rules using SwissADME

Molecules	MW (gm/mol)	NRB	HBA	HBD	TPSA (Å²)	Logp (clogp)	Lipinski's rule violation	Veber's rule violation
Quercetin	302.24	1	7	5	131.36	1.23	0	0
Ursolic acid	456.70	1	3	2	57.53	5.88	1	0
β-sitosterol	414.71	6	1	1	20.23	7.19	1	0
Berberine	336.4	2	4	0	40.80	2.53	0	0
Rutin	610.5	6	16	10	269.43	-1.29	3	1

The ADME (Absorption, Distribution, Metabolism, and Excretion) properties and physicochemical parameters of all selected ligands were systematically predicted using the pkCSM web server (https://biosig.unimelb.edu.au/pkcsm/), which applies graph-based signatures and machine learning models trained on experimentally validated datasets. The following pharmacokinetic parameters were evaluated: Absorption (human intestinal absorption 'HIA'), Distribution predicted (volume of distribution 'Vd'), and blood–

brain barrier (BBB) permeability, Metabolism; interaction potential with key cytochrome P450 isoenzymes to estimate metabolic stability, and Excretion (predicted total clearance and renal elimination profile Table 7. The SwissADME Bioavailability Radar for the Quercetin and Berberine, as they show good binding poses, evaluates six key physicochemical parameters—lipophilicity (LIPO), molecular size (SIZE), polarity (POLAR), solubility (INSOLU), saturation (INSATU), and molecular flexibility (FLEX) (Figure 5). Compounds falling within the predefined pink zone for these axes are predicted to possess favorable oral drug-likeness and membrane permeability. Collectively, these data allowed for a comparative assessment of the compounds' oral bioavailability and compliance with established drug-likeness guidelines. The BOILED-Egg model was used to predict gastrointestinal absorption (white region), brain penetration (yolk region), and P-glycoprotein substrate (PGP+/–) for Quercetin and Berberine. Quercetin is positioned within the white region, indicating high probability of gastrointestinal absorption (HIA) but low blood–brain barrier (BBB) permeability with P-glycoprotein substrate (PGP-). Berberine also shows good intestinal absorption but limited BBB penetration with P-glycoprotein substrate (PGP+). These predictions suggest both compounds are orally bioavailable but unlikely to cross the central nervous system barrier efficiently (Figure 6).

Table 7: Predicted ADME Properties of phytochemicals Using pkCSM

Compounds	Absorption			Distribution				Metabolism		Excretion	
	Water solubility (log mol/L)	HIA (% Absorbed)	Skin Permeability (log Kp)	VDss (human) (log L/kg)	Fraction unbound (human) (Fu)	BBB permeability (log BB)	CNS permeability (log PS)	CYP2D6 substrate CYP3A4 substrate CYP1A2 inhibitor CYP2C19 inhibitor CYP2C9 inhibitor CYP1A2 inhibitor CYP2D6 inhibitor		Total Clearance (log ml/min/kg)	Renal OCT2 substrate
Quercetin	-2.925	77.207	-2.735	1.559	0.206	-1.098	-3.065	No, (CYP1A2 inhibitor = yes)		0.407	No
Ursolic acid	-3.072	100	-2.735	-1.088	0	-0.141	-1.187	No, (CYP3A4 substrate = yes)		0.083	No
β-sitosterol	-6.773	94.464	-2.783	0.193	0	0.781	-1.705	No, (CYP3A4 substrate = yes)		0.628	No
Berberine	-3.973	97.147	-2.576	0.58	0.262	0.198	-1.543	No foe CYP2D6 substrate, CYP2C19 inhibitor, and CYP2C9 inhibitior		1.273	No
Rutin	-2.893	23.446	-2.735	1.663	0.187	-1.899	-5.178	No		-0.369	No

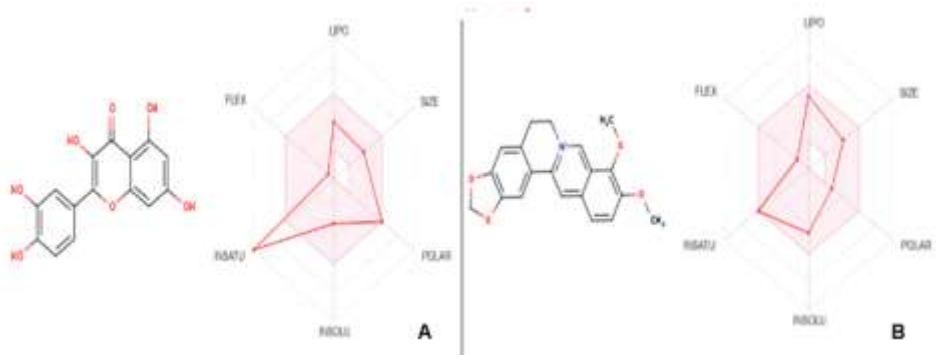

Figure 5: SwissADME Bioavailability Radar for the (A) Quercetin and (B) Berberine

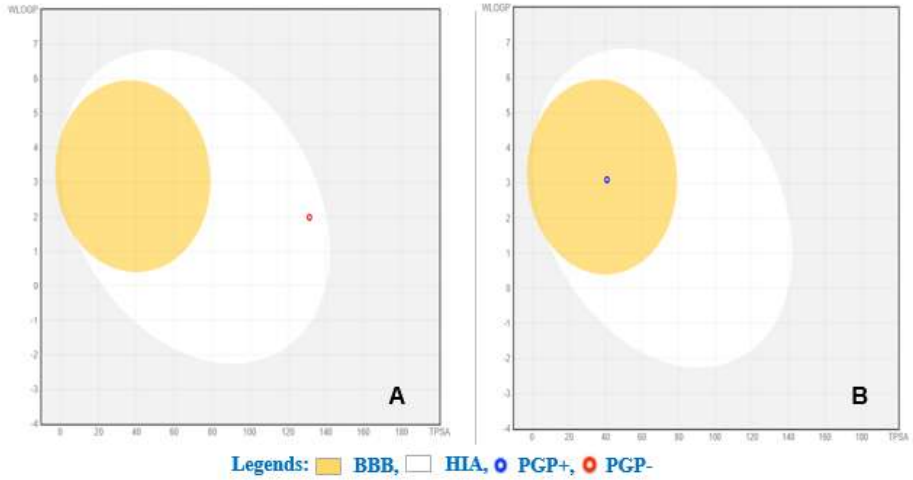

Figure 6: The BOILED-Egg c for the (A) Quercetin and (B) Berberine.

5. Toxicity Prediction

Toxicity profiles of the selected phytochemicals were predicted using Pro-Tox III. The model classified each of them based on LD_{50} estimates, its respective toxicity class, and organ toxicity, and is summarized in Table 8.

Table 8: Toxicity prediction of phytochemicals computed by Pro-Tox III.

Compounds	LD50 (mg/kg)	Toxicity class	Organ Toxicity				
			Hepatotoxicity	Carcinogenicity	Immunotoxicity	Mutagenicity	Cytotoxicity
Quercetin	159	3	Inactive	Active	Inactive	Active	Inactive
Ursolic acid	2000	4	Active	Active	Active	Inactive	Inactive
β-sitosterol	890	4	Inactive	Inactive	Active	Inactive	Inactive
Berberine	200	3	Inactive	Active	Active	Active	Active
Rutin	5000	5	Inactive	Inactive	Active	Inactive	Inactive

Discussion

1. Molecular Docking and Binding Affinity

Key Finding: Quercetin (-8.8 kcal/mol) and Berberine (-8.7 kcal/mol) exhibited the strongest predicted binding to the Androgen Receptor (AR) as shown in Table 9. The more negative the binding energy, the stronger the expected affinity. Anomaly: Ursolic acid showed a positive binding energy (+1 kcal/mol), indicating it is highly unfavorable to bind to the active site, suggesting a weak or non-existent interaction in this conformation. However, molecular docking provides a static representation of ligand–receptor interactions; therefore, further validation using

molecular dynamics simulations is recommended to evaluate the stability of these complexes under physiological conditions.

Table 9: Interpreted Binding Affinity

Ligand	Binding Energy (kcal/mol)	AR affinity (interpretation)
Quercetin	-8.8	Highest affinity/most favorable
Ursolic acid	1 (positive)	Very low/unfavorable
β-sitosterol	-6.1	Moderate affinity
Berberine	-8.7	Strong affinity
Rutin	-5.8	Lowest favorable affinity

2. Molecular Interactions

Quercetin demonstrated the strongest predicted binding affinity among the screened phytochemicals, primarily due to its capacity to form multiple stabilizing hydrogen bonds with key residues within the androgen receptor (AR) ligand-binding domain, including LEU704, ASN705, and MET745. These interactions are essential for anchoring the molecule within the binding cavity and likely contribute to its favorable conformational stability and interaction energy. This binding profile supports a mechanistic hypothesis in which Quercetin may effectively modulate AR activity through a combination of hydrogen bonding and complementary hydrophobic contacts.

Berberine exhibited the second-highest affinity toward AR, characterized by a notable hydrogen bond with ARG752, a residue commonly implicated in ligand stabilization and receptor modulation processes. Although its interaction network is less extensive than that of Quercetin, the presence of this key H-bond, along with supportive van der Waals and electrostatic interactions, indicates a meaningful binding mode that may permit partial modulation of the receptor. Together, these interaction patterns highlight Quercetin as a potentially superior AR modulator, with Berberine exhibiting a comparatively moderate yet structurally relevant binding behavior. Conversely, the remaining phytochemicals—Ursolic acid, β-sitosterol, and Rutin—exhibited comparatively weak or non-optimal interactions within the AR binding pocket. Their docking poses showed limited hydrogen bonding capacity and suboptimal alignment with key functional residues, resulting in reduced binding affinities and less stable conformational fits. These findings suggest that, despite their biological relevance, these compounds are unlikely to exert meaningful modulatory effects on the androgen receptor under the conditions evaluated.

3. Drug-likeness and Pharmacokinetics (ADME)

In terms of lead identification, both Quercetin and Berberine comply with Lipinski's and Veber's criteria, supporting their classification as orally bioavailable, drug-like candidates. In contrast, Rutin is unlikely to demonstrate effective oral activity because of its substantial molecular size and pronounced polarity (TPSA 269.43 Å²), which markedly limit membrane permeability. Additionally, although Ursolic acid and β-sitosterol exhibit high LogP values indicative of poor aqueous solubility, their strong lipophilicity suggests the potential for adequate membrane interaction and passive permeability, as summarized in Table 10.

Table 10: Lipinski's and Veber's rules interpretation

Molecule	Lipinski Violations	Veber Violations	Notes
Quercetin	0	0	Excellent drug-likeness
Ursolic acid	1 (Logp)	0	High lipophilicity (Logp: 5.88)
β-sitosterol	1 (Logp)	0	Very high lipophilicity (Logp: 7.19)
Berberine	0	0	Excellent drug-likeness.
Rutin	3 (MW, HBA, TPSA)	1 (TPSA)	Very large and polar; poor oral potential

HIA: Quercetin, Ursolic acid, Beta-sitosterol, and Berberine show excellent predicted Human Intestinal Absorption (HIA). Rutin's HIA is poor, consistent with its poor drug-likeness. Metabolism profiling indicated compound-specific interactions with the CYP3A4 enzyme system. Quercetin was predicted to exhibit neither substrate nor inhibitory activity toward CYP3A4, suggesting a minimal risk of CYP3A4-mediated drug–drug interactions. In contrast, Berberine was identified as a CYP3A4 substrate, indicating potential susceptibility to metabolic clearance via this pathway. Likewise, Ursolic acid and Beta-sitosterol were also predicted to act as CYP3A4 substrates, whereas Rutin demonstrated no interaction with the enzyme. Collectively, these findings suggest that CYP3A4-mediated metabolism may play a role in the pharmacokinetic behavior of selected phytochemicals, while the absence of inhibitory activity reduces the likelihood of enzyme-mediated drug–drug interactions, as shown in Table 11.

Table 11: ADME Properties of selected phytochemicals

Compound	HIA (%)	BBB Permeability	CYP3A4 Substrate/Inhibitor
Quercetin	77.207(Good)	Low (-1.098)	Neither of Both
Ursolic acid	100 (Very Good)	Moderate (-0.141)	Substrate
β-sitosterol	94.464(Very Good)	Permeable (0.781)	Substrate
Berberine	97.147(Very Good)	Permeable (0.198)	Substrate
Rutin	23.446 (Poor)	Very Low (-1.899)	None

Quercetin's bioavailability radar suggests generally acceptable physicochemical properties, including molecular size, flexibility, and lipophilicity, and it is predicted to be a non-substrate of P-glycoprotein (P-gp–). However, it deviates from optimal ranges in aqueous solubility and exhibits low saturation (fraction of sp^3 carbons), reflecting its planar structure. Among these factors, poor aqueous solubility and extensive metabolic conjugation are likely the primary contributors to its limited oral bioavailability. Consequently, formulation strategies such as nanosuspensions, prodrug design, or complexation approaches may be required to enhance its pharmacokinetic performance. Although berberine's physicochemical profile (molecular size, flexibility, lipophilicity, aqueous solubility, as well as saturation) could fall largely within SwissADME 's acceptable radar ranges, its documented poor oral bioavailability *in vivo* — largely due to P-glycoprotein efflux and extensive first-pass metabolism- underscores the need for formulation approaches to enhance *in vivo* availability. BOILED-Egg modeling predicted that Quercetin exhibits high gastrointestinal absorption (white region) but low blood–brain barrier (BBB) penetration (yolk region). Berberine is predicted to exhibit moderate intestinal permeability based on in silico models; however, its actual oral absorption in vivo is markedly limited due to active efflux by P-glycoprotein and extensive first-pass metabolism. Additionally, it demonstrates low blood–brain barrier permeability, indicating restricted central nervous system penetration; however, Quercetin is classified as a P-glycoprotein substrate (PGP-), whereas Berberine is not (PGP+). In the intestine, P-glycoprotein can limit oral absorption, while at the blood–brain barrier, it restricts the entry of substrate compounds into the central nervous system. However, Quercetin is predicted to be a non-substrate of P-glycoprotein and has been reported to inhibit its activity. Therefore, it is unlikely to experience significant efflux-related limitations and may instead enhance the intracellular retention of co-administered P-glycoprotein substrates.

4.Toxicity Prediction

Quercetin and Berberine were classified as toxicity class 3, the lowest predicted toxicity among evaluated phytochemicals, indicating moderate acute toxicity, with predicted carcinogenicity and mutagenicity for both compounds; additionally, Berberine exhibited cytotoxicity and immunotoxicity. Ursolic acid and β-sitosterol were assigned to toxicity class 4, corresponding to low acute toxicity, with Ursolic acid showing hepatotoxicity, carcinogenicity, and immunotoxicity, and β-sitosterol displaying immunotoxicity potential. Rutin demonstrated the low predicted toxicity (class 5) and was largely inactive across the evaluated organ toxicity endpoints, except for immunotoxicity Table 12

Table 12: LD_{50} and Toxicity Class of selected phytochemicals

Compound	LD_{50} (mg/kg)	Toxicity Class
Quercetin	159	3 (Toxic)
Ursolic acid	2000	4 (Harmful)
β-sitosterol	890	4 (Harmful)
Berberine	200	3 (Toxic)
Rutin	5000	5 (Low Toxicity)

Conclusion

The integrated application of molecular docking, ADMET, and drug-likeness analyses enabled a robust prioritization of phytochemicals targeting the androgen receptor. Quercetin and Berberine demonstrated the most favorable profiles, exhibiting strong binding affinities, compliance with key drug-likeness rules, and acceptable pharmacokinetic properties. In contrast, Rutin showed poor binding and unfavorable ADMET characteristics, limiting its therapeutic potential. Overall, Quercetin emerged as the most promising candidate based on *in silico* predictions, warranting further experimental validation. These findings highlight the value of integrated *in silico* approaches in rational drug discovery.

Compliance with ethical standards:

This study was conducted using computational methods only and did not involve human participants, clinical data, or experimental animals; therefore, ethical approval and informed consent were not required.

Compliance with ethical standards

Disclosure of conflict of interest

The authors declare that they have no conflict of interest.

References

[1] K. Pereira de Jésus-Tran, P. L. Côté, L. Cantin, J. Blanchet, F. Labrie, and R. Breton, "Comparison of crystal structures of human androgen receptor ligand-binding domain complexed with various agonists reveals molecular determinants responsible for binding affinity," (in eng), Protein Sci, vol. 15, no. 5, pp. 987-99, May 2006, doi: 10.1110/ps.051905906.

[2] G. Van-Duyne, I. A. Blair, C. Sprenger, V. Moiseenkova-Bell, S. Plymate, and T. M. Penning, "The androgen receptor," (in eng), Vitam Horm, vol. 123, pp. 439-481, 2023, doi: 10.1016/bs.vh.2023.01.001.

[3] R. A. Davey and M. Grossmann, "Androgen Receptor Structure, Function and Biology: From Bench to Bedside," (in eng), Clin Biochem Rev, vol. 37, no. 1, pp. 3-15, Feb 2016.

[4] G. Aurilio et al., "Androgen Receptor Signaling Pathway in Prostate Cancer: From Genetics to Clinical Applications," (in eng), Cells, vol. 9, no. 12, Dec 10 2020, doi: 10.3390/cells9122653.

[5] E. Likos, A. Bhattarai, C. M. Weyman, and G. C. Shukla, "The androgen receptor messenger RNA: what do we know?," (in eng), RNA Biol, vol. 19, no. 1, pp. 819-828, Jan 2022, doi: 10.1080/15476286.2022.2084839.

[6] M. Akhtar, K. Murshed, Noheir, H. Telfah, and I. Albozom, "Role of Androgen Receptor in Prostate Cancer: A Brief Update," Journal on oncology, vol. 4, p. 1142, 08/26 2024, doi: 10.52768/2692-563X/1142.

[7] F. Chen et al., "Computational analysis of androgen receptor (AR) variants to decipher the relationship between protein stability and related-diseases," (in eng), Sci Rep, vol. 10, no. 1, p. 12101, Jul 21 2020, doi: 10.1038/s41598-020-68731-7.

[8] A. Meszaros, J. Ahmed, G. Russo, P. Tompa, and T. Lazar, "The evolution and polymorphism of mono-amino acid repeats in androgen receptor and their regulatory role in health and disease," (in eng), Front Med (Lausanne), vol. 9, p. 1019803, 2022, doi: 10.3389/fmed.2022.1019803.

[9] D. Özturan, T. Morova, and N. A. Lack, "Androgen Receptor-Mediated Transcription in Prostate Cancer," Cells, vol. 11, no. 5, p. 898, 2022. [Online]. Available: https://www.mdpi.com/2073-4409/11/5/898.

[10] S. Wen, Y. Niu, and H. Huang, "Posttranslational regulation of androgen dependent and independent androgen receptor activities in prostate cancer," (in eng), Asian J Urol, vol. 7, no. 3, pp. 203-218, Jul 2020, doi: 10.1016/j.ajur.2019.11.001.

[11] L. E. V. Lumahan, M. Arif, A. E. Whitener, and P. Yi, "Regulating Androgen Receptor Function in Prostate Cancer: Exploring the Diversity of Post-Translational Modifications," (in eng), Cells, vol. 13, no. 2, Jan 19 2024, doi: 10.3390/cells13020191.

[12] F. Raith, D. H. O'Donovan, C. Lemos, O. Politz, and B. Haendler, "Addressing the Reciprocal Crosstalk between the AR and the PI3K/AKT/mTOR Signaling Pathways for Prostate Cancer Treatment," International Journal of Molecular Sciences, vol. 24, no. 3, p. 2289, 2023. [Online]. Available: https://www.mdpi.com/1422-0067/24/3/2289.

[13] M. Hashemi et al., "Targeting PI3K/Akt signaling in prostate cancer therapy," (in eng), J Cell Commun Signal, vol. 17, no. 3, pp. 423-443, Sep 2023, doi: 10.1007/s12079-022-00702-1.

[14] G. N. Fanelli, P. V. Nuzzo, F. Pederzoli, and M. Loda, "Deciphering Complexity: The Molecular Landscape of Castration-Resistant Prostate Cancer," Surgical Pathology Clinics, vol. 18, no. 1, pp. 25-39, 2025/03/01/ 2025, doi: https://doi.org/10.1016/j.path.2024.10.003.

[15] N. Wüstmann et al., "Co-expression and clinical utility of AR-FL and AR splice variants AR-V3, AR-V7 and AR-V9 in prostate cancer," Biomarker Research, vol. 11, no. 1, p. 37, 2023/04/05 2023, doi: 10.1186/s40364-023-00481-w.

[16] D. Han et al., "Androgen receptor splice variants drive castration-resistant prostate cancer metastasis by activating distinct transcriptional programs," (in eng), J Clin Invest, vol. 134, no. 11, Apr 30 2024, doi: 10.1172/jci168649.

[17] L. Yin, S. Qi, and Z. Zhu, "Advances in mitochondria-centered mechanism behind the roles of androgens and androgen receptor in the regulation of glucose and lipid metabolism," (in eng), Front Endocrinol (Lausanne), vol. 14, p. 1267170, 2023, doi: 10.3389/fendo.2023.1267170.

[18] Q. Liu, X. Yin, and P. Li, "Clinical characteristics, AR gene variants, and functional domains in 64 patients with androgen insensitivity syndrome," Journal of Endocrinological Investigation, vol. 46, no. 1, pp. 151-158, 2023/01/01 2023, doi: 10.1007/s40618-022-01894-4.

[19] A. Gromova et al., "X-linked SBMA model mice display relevant non-neurological phenotypes and their expression of mutant androgen receptor protein in motor neurons is not required for neuromuscular disease," Acta Neuropathologica Communications, vol. 11, no. 1, p. 90, 2023/06/02 2023, doi: 10.1186/s40478-023-01582-1.

[20] C. Marchioretti, R. Andreotti, E. Zuccaro, A. P. Lieberman, M. Basso, and M. Pennuto, "Spinal and bulbar muscular atrophy: From molecular pathogenesis to pharmacological intervention targeting skeletal muscle," (in eng), Curr Opin Pharmacol, vol. 71, p. 102394, Aug 2023, doi: 10.1016/j.coph.2023.102394.
[21] M. Ehsani, F. O. David, and A. Baniahmad, "Androgen Receptor-Dependent Mechanisms Mediating Drug Resistance in Prostate Cancer," (in eng), Cancers (Basel), vol. 13, no. 7, Mar 26 2021, doi: 10.3390/cancers13071534.
[22] C. Rodriguez Tirado et al., "UBE2J1 is the E2 ubiquitin-conjugating enzyme regulating androgen receptor degradation and antiandrogen resistance," (in eng), Oncogene, vol. 43, no. 4, pp. 265-280, Jan 2024, doi: 10.1038/s41388-023-02890-5.
[23] M. Azeem, M. Hanif, K. Mahmood, N. Ameer, F. R. S. Chughtai, and U. Abid, "An insight into anticancer, antioxidant, antimicrobial, antidiabetic and anti-inflammatory effects of quercetin: a review," (in eng), Polym Bull (Berl), vol. 80, no. 1, pp. 241-262, 2023, doi: 10.1007/s00289-022-04091-8.
[24] M. J. Saadh et al., "Therapeutic effects of quercetin in oral cancer therapy: a systematic review of preclinical evidence focused on oxidative damage, apoptosis and anti-metastasis," Cancer Cell International, vol. 25, no. 1, p. 66, 2025/02/24 2025, doi: 10.1186/s12935-025-03694-1.
[25] M. Zhao et al., "Anti-inflammatory and antioxidant activity of ursolic acid: a systematic review and meta-analysis," (in eng), Front Pharmacol, vol. 14, p. 1256946, 2023, doi: 10.3389/fphar.2023.1256946.
[26] B. D. Besasie, A. Saha, J. DiGiovanni, and M. A. Liss, "Effects of curcumin and ursolic acid in prostate cancer: A systematic review," (in eng), Urologia, vol. 91, no. 1, pp. 90-106, Feb 2024, doi: 10.1177/03915603231202304.
[27] A. Manal, "Ursolic acid alleviates isoproterenol-induced kidney injury in mice by suppressing inflammation, apoptosis, and oxidative stress via the PI3K/Akt signaling," Asian Pacific Journal of Tropical Biomedicine, vol. 15, no. 8, pp. 324-332. [Online]. Available: apjtb/article/abstract/20250803.
[28] Y. Wu et al., "The active ingredient β-sitosterol in the anti-inflammatory agents alleviates perianal inflammation in rats by inhibiting the expression of Srebf2, activating the PPAR signaling pathway, and altering the composition of gut microbiota," International Immunopharmacology, vol. 152, p. 114470, 2025/04/16/ 2025, doi: https://doi.org/10.1016/j.intimp.2025.114470.
[29] H. Wang, Z. Wang, Z. Zhang, J. Liu, and L. Hong, "β-Sitosterol as a Promising Anticancer Agent for Chemoprevention and Chemotherapy: Mechanisms of Action and Future Prospects," (in eng), Adv Nutr, vol. 14, no. 5, pp. 1085-1110, Sep 2023, doi: 10.1016/j.advnut.2023.05.013.
[30] S. A. Kan et al., "β-sitosterol suppresses fibroblast growth factor and epidermal growth factor receptors to induce apoptosis and inhibit migration in lung cancer: an in vitro study," (in eng), Am J Cancer Res, vol. 15, no. 3, pp. 1109-1121, 2025, doi: 10.62347/nzcg1179.
[31] R.-G. Xiong et al., "Anticancer Effects and Mechanisms of Berberine from Medicinal Herbs: An Update Review," Molecules, vol. 27, no. 14, p. 4523, 2022. [Online]. Available: https://www.mdpi.com/1420-3049/27/14/4523.
[32] J. Wang, C. Bi, H. Xi, and F. Wei, "Effects of administering berberine alone or in combination on type 2 diabetes mellitus: a systematic review and meta-analysis," (in eng), Front Pharmacol, vol. 15, p. 1455534, 2024, doi: 10.3389/fphar.2024.1455534.
[33] G. Shams, S. Abd Allah, and R. Ezzat, "Pharmacological activities and medicinal uses of berberine: A review," Journal of Advanced Veterinary Research, vol. 14, no. 2, pp. 330-334, 02/09 2024. [Online]. Available: https://www.advetresearch.com/index.php/AVR/article/view/1515.
[34] S. M. Saafan et al., "Rutin attenuates D-galactose-induced oxidative stress in rats' brain and liver: molecular docking and experimental approaches," (in eng), Food Funct, vol. 14, no. 12, pp. 5728-5751, Jun 19 2023, doi: 10.1039/d2fo03301a.
[35] A. Muhammad et al., "An Overview of Anticancer, Anti-inflammatory, Antioxidant, Antimicrobial, Cardioprotective, and Neuroprotective Effects of Rutin," Currents in Pharmaceutical Research, vol. 2, no. 2, 11/15 2024, doi: 10.32350/cpr.22.06.

